

Large- n $O(n)$ with long-range interactions: integrability and resonance dynamics

Guido Giachetti¹ and Nicolò Defenu^{2,3}

¹*Laboratoire de Physique de l’École Normale Supérieure, CNRS, ENS & PSL University, Sorbonne Université, Université Paris Cité, 75005 Paris, France*

²*Institut für Theoretische Physik, ETH Zürich, Wolfgang-Pauli-Str. 27 Zürich, Switzerland*

³*CNR-INO, Area Science Park, Basovizza, I-34149 Trieste, Italy*

We study the the large- n dynamics of the long-range quantum $O(n)$ model, focusing on the strong long-range regime $\alpha < d$. The dynamics of the model exhibits non-trivial features on mesoscopic timescales $t \sim \ln N$, due to the activation of parametric resonances of the nearly degenerate quantum modes. By using recent results establishing the integrability of the large- n limit, we derive the resonance conditions, and construct the reduced multi-mode Hamiltonian that captures the finite-size dynamics. This framework yields the resonance phase diagram and clarifies when and how deviations from mean-field behavior arise. In particular, the presence of multiple resonant modes enhances the logarithmic growth of entanglement and leads to spatially modulated correlations.

I. INTRODUCTION

Within the framework of statistical mechanics and condensed matter physics, it is well established that long-range (LR) interactions—i.e., slowly decaying power-law couplings—can give rise to a wealth of novel phenomena in both equilibrium and non-equilibrium regimes, for classical [1] as well as quantum [2, 3] systems. This topic has recently attracted renewed attention, largely due to the increasing feasibility of experimental realizations in atomic, molecular, and optical (AMO) platforms [2, 4–10]. These advances have unveiled a rich phenomenology, including dynamical phase transitions [11, 12], exotic quantum phases [13, 14], and modified universal defect-scaling laws [15, 16]. In particular, the dynamical behavior of LR systems has sparked intense interest in recent years, owing to their intrinsic tendency to avoid equilibration [3, 17–19]. This lack of thermalization plays a crucial role in stabilizing non-equilibrium many-body phases, such as discrete and higher-order time crystals [20–22].

Within this context, the d -dimensional $O(n)$ model—long regarded as a cornerstone of out-of-equilibrium field theory [23–28]—provides an ideal framework to investigate the impact of long-range interactions. Its critical behavior depends crucially on the spatial decay of the coupling, $J(r) \sim r^{-\alpha}$, where r denotes the distance between lattice sites. In particular, a threshold value $\sigma^* > 0$ exists such that, for $\alpha > d + \sigma^*$, the finite-temperature criticality falls within the short-range universality class, whereas for $d < \alpha < d + \sigma^*$ [29–32]—the so-called weak long-range regime [33]—the critical exponents become α -dependent. The threshold σ^* increases from $\sigma^* = 1$ in $d = 1$ [30, 34–38] to $\sigma^* = 2$ for $d \geq 4$ [29–31, 39], exhibiting a nontrivial dependence on n in intermediate dimensions [31, 40]. Analogous results hold for quantum critical points at zero temperature, whose universal properties are connected to those of anisotropic long-range models via the quantum-to-classical correspondence [41, 42]. More generally, the leading-order scaling behavior in the weak long-range regime can be mapped to that of local systems in higher (fractional) effective dimensions [30, 31, 43].

In the strong long-range regime, $\alpha < d$ [3], the model displays a striking non-equivalence between descriptions based on different statistical mechanics ensembles [1, 44, 45]. The question of how ensemble inequivalence manifests in the quantum regime has recently attracted growing attention [46], following the pioneering investigations of Ref. [45, 47].

Similarly, the quantum dynamics of the $O(n)$ model far from equilibrium has been widely studied in the large- n limit [48]. In this regime, depending on the initial state of the dynamics, the problem can be solved exactly [25, 27, 28] and is described by the spherical model [49, 50]. The large- n quantum dynamics displays a rich and complex behavior, already for local interactions, including dynamical phase transitions [51–53], coarsening processes [51–53] and aging phenomena [54].

Ref. [55] investigated the large- n dynamics in the strong long-range regime, showing that large- n $O(n)$ models can be interpreted as an interplay between a classical mean-field degree of freedom—whose oscillations remain undamped—and several quantum bosonic modes responsible for spreading quantum correlations. Although these correlations are suppressed as the system size N grows, parametric resonances in the semiclassical dynamics can amplify them on a mesoscopic timescale $t_{\text{Ehr}} \sim \ln N$, during which genuinely quantum effects such as entanglement production occur. Many of these features are shared by other strong long-range models, including long-lived prethermal states [17, 19], persistent oscillations [56–59], and anomalous entanglement spreading [60, 61]. However, the relative simplicity of the large- n model enables a semi-analytical description of these phenomena, providing a paradigmatic framework for understanding strong long-range dynamics.

In this paper, we extend the understanding of $O(n)$ dynamics by generalizing the results of Ref. [62], which introduced a new formalism to describe the model's integrable dynamics, to the strong long-range regime. Our approach provides fresh insights into this problem, enabling us to develop a quantitative framework that supports the predictions of Ref. [55] and, in doing so, offers a comprehensive and coherent picture of the underlying physics.

The paper is organized as follows. In Sec. II, we introduce the model and discuss the large- n limit. Sec. III analyzes the thermodynamic limit, $N \rightarrow \infty$, where the dynamics is dominated by the classical mean-field degree of freedom. In Sec. IV, we present the integrals of motion that allow us to describe the dynamics even at finite (but large) N . Specifically, Sec. V focuses on the linear stability analysis, identifying the conditions under which quantum modes become resonant and constructing the corresponding phase diagram. Sec. VI then investigates the fate of these resonant modes by deriving a reduced Hamiltonian and computing its spectrum exactly. Finally, in Sec. VII, we revisit the role of resonances in entanglement production and provide semi-quantitative expressions for the entanglement entropy. In particular, we show that in the multi-resonant case—where more than one quantum mode becomes resonant—the entanglement spreading is significantly enhanced, a phenomenon we relate to the breaking of the model's effective permutational symmetry.

II. THE MODEL

We introduce here the quantum $O(n)$ model and discuss the effect of long-range interactions. Without loss of generality, we can restrict ourselves to the $d = 1$ case. We thus consider a quantum chain with N sites: each site j corresponds to a vector variable of bosonic components $n \Phi_j$ and its conjugate momentum Π_j ($[\Phi_j^a, \Pi_{j'}^{a'}] = i \delta_{r,r'} \delta_{j,j'}$, with $a, a' = 1, \dots, n$). The dynamics of the model is given by a long-range quadratic hopping and a local, $O(n)$ -symmetric, quartic potential

$$H = \sum_j \frac{1}{2} \Pi_j^2 + \frac{1}{2N_\alpha} \sum_{j \neq j'} \frac{(\Phi_j - \Phi_{j'})^2}{|j - j'|^\alpha} + \sum_j \frac{r}{2} \Phi_j^2 + \frac{\lambda}{2n} (\Phi_j^2)^2. \quad (1)$$

Here r represents the bare mass of the theory, $\lambda > 0$ the quartic $O(n)$ coupling, $\alpha > 0$ the decay exponent of the interaction and $N_\alpha = \sum_{j>0} j^{-\alpha}$ is the Kac scaling [63]. Let us notice that, while for $\alpha > 1$, N_α just fixes the energy scale of the excitation, for $\alpha < 1$ its presence is fundamental to ensure the extensivity of the thermodynamic quantities [1].

The range of the interaction can be tuned between the nearest-neighbors limit ($\alpha = \infty$) and the fully connected limit ($\alpha = 0$). For $\alpha > 3$ the hopping term can be seen as a discretized version of the Laplacian operator, so that Hamiltonian (1) is the lattice version of the usual short-range $O(n)$ bosonic field theory. For $\alpha < 3$, the ground state of the model undergoes a transition between a massive ($\langle \Phi \rangle \neq 0$) and a massless ($\langle \Phi \rangle = 0$) phase [41], where $\langle \cdot \rangle$ denotes the expectation value over a quantum state. We will consider the following protocol: for $t < 0$, we choose $r^- > 0$, and assume the system to be in its massless ground state; then at $t = 0$ the bare mass is quenched to its (possibly negative) final value r . In particular, here we will focus on the strong-long-range regime $\alpha < 1$.

The dynamics of the model becomes tractable in the limit $n \rightarrow \infty$, under the condition that the initial state is factorized and homogeneous over both the lattice and the component indices [64]: in this case, for $n \rightarrow \infty$, such a factorization is maintained at any time t , so that it is possible to replace $\Phi_j^2 \Phi_j^a \rightarrow n \langle \Phi_a^2 \rangle \Phi_j^2$ in the Heisenberg equations of motion (e.o.m.) coming from Eq. (1).

In the large- n limit the e.o.m. can thus be written explicitly in Fourier space

$$\dot{\Phi}_k = \Pi_k^\dagger, \quad \dot{\Pi}_k = -(r + \lambda \langle \Phi^2 \rangle + \omega_k^2) \Phi_k^\dagger, \quad (2)$$

as each component evolves identically and independently from the others, the internal field index $a \in \{1, \dots, n\}$ has been dropped. Here $k = 2\pi\nu/N$, $\nu = -N/2 + 1, \dots, N/2$ and

$$\Phi_k = \frac{1}{\sqrt{N}} \sum_j e^{ikj} \Phi_j \quad \Pi_k = \frac{1}{\sqrt{N}} \sum_j e^{-ikj} \Pi_j \quad (3)$$

are the bosonic Fourier modes ($[\Phi_k, \Pi_{k'}] = i \delta_{k'k}$); ω_k^2 is the lattice dispersion relation

$$\omega_k^2 = \frac{1}{2N_\alpha} \sum_{j>0} \frac{1 - \cos(kj)}{j^\alpha}. \quad (4)$$

Physically speaking, we can interpret the system of Eq. (2) as a collection of N bosons, coupled through a collective, time-dependent, classical degree of freedom

$$m^2(t) = r + \lambda \langle \Phi^2 \rangle = r + \frac{\lambda}{N} \sum_k \langle \Phi_k^\dagger \Phi_k \rangle \quad (5)$$

which plays the role of the renormalized mass. For constant m , the system reduces to a set of independent bosonic modes, but for a time-dependent $m(t)$, the occupation number of the modes may change and scattering occurs. Notice that $m^2(t)$ need not be positive at any time, while $m^2(t) \geq 0$ in any stationary state.

The dramatic simplification at the level of the dynamics can be appreciated by noticing that the time-evolution of second order correlators can be cast in terms of a closed set of ODE. In particular, if we parameterize the second order moments as $|\eta_k|^2 \equiv \langle \Phi_k^\dagger \Phi_k \rangle$, $2\Re(\eta_k^* p_k) \equiv \langle \Pi_k \Phi_k + \text{h.c.} \rangle$, $|p_k|^2 \equiv \langle \Pi_k^\dagger \Pi_k \rangle$, the e.o.m. (2) become

$$\dot{\eta}_k = p_k, \quad \dot{p}_k = - \left(r + \omega_k^2 + \frac{\lambda}{N} \sum_k |\eta_k|^2 \right) \eta_k. \quad (6)$$

These equations can be derived from the classical Hamiltonian

$$\mathcal{H} = \frac{1}{2} \sum_k (|p_k^2| + (r + \omega_k^2) |\eta_k^2|) + \frac{\lambda}{4N} \left(\sum_k |\eta_k^2| \right)^2. \quad (7)$$

Let us notice that the range of the interaction enters the e.o.m. and Eq. (7) only through the dispersion ω_k : in particular, the local field theory limit is recovered by inserting the dispersion relation $\omega_k \sim k$ in Eqs. (2) and (6). On the other hand, for $0 < \alpha < 1$ instead, the spectrum remains discrete even in the thermodynamic limit [19] and it is more conveniently parameterized by the integer index ν . In particular, the eigenvalues accumulate around $\omega_\infty^2 = 1$ as

$$\omega_\nu^2 = 1 - (1 - \alpha) \pi^{\alpha-1} \int_0^\pi dx \frac{\cos(\nu x)}{x^\alpha} \quad (8)$$

while $\omega_0 = 0$ as required by the translational invariance of the model. In the $\alpha = 0$ limit, we have $\omega_\nu = 1 - \delta_{\nu,0}$, so that we have an almost perfect degeneracy broken only by the zero mode, in agreement with the perfect permutational symmetry of the model.

III. THERMODYNAMIC LIMIT

The peculiar form of the dispersion of the excitations ω_ν in Eq. (8) in the strong-long-range regime leads to several simplification of the problem in the thermodynamic $N \rightarrow \infty$. Indeed, as a growing fraction of the modes lies arbitrarily close to $\omega_\infty = 1$, for any global operator G one has

$$\lim_{N \rightarrow \infty} \frac{1}{N} \sum_\nu G(\omega_\nu^2) = G(1) + O(N^{-\zeta}), \quad (9)$$

provided that $G(\omega_\nu) = O(1)$ for all ν . As shown in Ref. [55], the order of the correction ζ is given by $\zeta = \max(\alpha, 1 - \alpha)$.

As a consequence, if one assume that $\eta_\nu = O(1)$ for all ν , one has that the only relevant degree of freedom is $\bar{\eta} = \eta_\infty$, $\bar{p} = p_\infty$, so that the classical Hamiltonian in Eq. (7) simplifies into

$$\epsilon = \lim_{N \rightarrow \infty} \frac{1}{N} \mathcal{H} = \frac{1}{2} |\bar{p}|^2 + \frac{1}{2} (r + 1) |\bar{\eta}|^2 + \frac{\lambda}{4} |\bar{\eta}|^4, \quad (10)$$

i.e. the Hamiltonian of a particle into a 2-dimensional quartic central potential. It is convenient to reparametrize the accumulation point coordinate $\bar{\eta} = \xi e^{i\theta}$, with the constraint $\xi^2 \dot{\theta} = \ell$ with $\ell \geq 1/2$ a constant. Then, we can write

$$\ell = \xi^2 \dot{\theta} \quad \epsilon = \frac{1}{2} \xi^2 + \frac{\ell^2}{2\xi^2} + \frac{1}{2} (r + 1) \xi^2 + \frac{\lambda}{4} \xi^4 \equiv \frac{1}{2} \dot{\xi}^2 + U_{\text{eff}}(\xi). \quad (11)$$

Note that $m^2 = r + \lambda \xi^2$, so that $m(t)$ is periodic, with a period that will be denoted as τ . The angular variable θ , is also periodic with a different frequency.

The variables $\bar{\eta}$ (or equivalently ξ, θ), can be physically interpreted as effective on-site degrees of freedom that capture the mean-field dynamics of the system. Indeed, any configuration with $\eta_\nu \rightarrow \bar{\eta}$, corresponds in real space to a set of ultra-local correlation functions

$$\langle \Phi_j \Phi_{j'} \rangle = \frac{1}{N} \sum_\nu \eta_\nu e^{ikj} \sim \bar{\eta} \delta_{j'j}. \quad (12)$$

The thermodynamic limit can thus be interpreted as a mean-field limit in which correlations between different sites are suppressed.

A. Initial conditions

For quantum quenches initialized in the system ground-state, i.e. a protocol where $r^- \rightarrow r$, the initial conditions of the classical variable $\bar{\eta}$ can be linked to the ground-state properties of the model with $r = r^-$. One has

$$\langle \Phi_\nu(0) \Phi_\nu(0)^\dagger \rangle = \frac{1}{2} (\omega_\nu^2 + m_{\text{gs}}^2)^{-1/2}, \quad \langle \Pi_\nu(0) \Pi_\nu(0)^\dagger \rangle = \frac{1}{2} (\omega_\nu^2 + m_{\text{gs}}^2)^{1/2}, \quad \langle \Phi_\nu(0) \Pi_\nu(0) \rangle = \frac{i}{2} \quad (13)$$

m_{gs} being the ground-state mass (to be determined), so that, up to immaterial phase factors,

$$\bar{\eta}(0) = \frac{1}{\sqrt{2}} (m_{\text{gs}}^2 + 1)^{-1/4}, \quad \bar{p}(0) = \frac{i}{\sqrt{2}} (m_{\text{gs}}^2 + 1)^{1/4} \quad (14)$$

and $\ell = 1/2$. Finally m_{gs} can be fixed through the equation $m = r^- + \lambda \xi^2$, which gives the self consistent condition

$$m_{\text{gs}}^2 = r_- + \frac{\lambda}{2} (m_{\text{gs}}^2 + 1)^{-1/2}. \quad (15)$$

In terms of the single degree of freedom ξ, θ these considerations have a transparent physical interpretation, as

$$\xi^2(0) = \frac{1}{2} (m_{\text{gs}}^2 + 1)^{-1/2}, \quad \dot{\xi}(0) = 0. \quad (16)$$

corresponds to the minimum of the effective radial potential $U_{\text{eff}}(\xi)$ in Eq. (11) for $r = r^-$. Let us notice that Eq. (15) predicts $m_{\text{gs}} \rightarrow 0$ is $r_- \rightarrow r_{\text{gs}}^c = -\lambda/2$, signaling the onset of a quantum phase transition, characterized by the condensation of one of the modes Φ^α which spontaneously breaks the $O(n)$ symmetry of the model.

IV. FINITE- N INTEGRABILITY

Although in the strict thermodynamic limit the dynamics of the model is characterized by the single degree of freedom $\bar{\eta}$ [55] a rich dynamical landscape can emerge on mesoscopic timescales $\ln N$, which remain accessible for realistic N . Indeed, for large but finite N the equation of motions can be written as

$$\ddot{\eta}_\nu = -(r + \omega_\nu^2 + \lambda |\bar{\eta}^2|) \eta_\nu + O(N^{-\zeta}) \quad (17)$$

For small times, the classical degree of freedom satisfies $|\bar{\eta}(t)| = \xi(t)$, which acts as a periodic forcing with period τ , determined by the solution of Eq. (11). Consequently, Eq. (17) takes the form of a Floquet–Hill equation. If the equation is not resonant, then $\eta_\nu = O(1)$, and the mean-field approximation remains valid over an interval that scales polynomially with the size of the system $O(N^\zeta)$. Conversely, if a parametric resonance occurs, then $\eta_\nu(t) \sim e^{\lambda_\nu t}$ and the single-mode approximation breaks down already at a timescale $t \sim (2\lambda_\nu)^{-1} \ln N$, since the finite size fluctuations acquire a macroscopic population $\eta_\nu^2(t) = O(N)$.

The condition under which the resonance occurs and the fate of the resonant degrees of freedom can be understood by noticing that the finite N dynamics is integrable [62]. Indeed, Eq. (7) can be rewritten in terms of the discrete dispersion relation ω_ν in Eq. (8), yielding

$$\mathcal{H} = \frac{1}{2} \sum_\nu (|p_\nu^2| + (r + \omega_\nu^2) |\eta_\nu^2|) + \frac{\lambda}{4N} \left(\sum_\nu |\eta_\nu^2| \right)^2. \quad (18)$$

We will now show that, for any N , one can write down a complete set of integrals of motions.

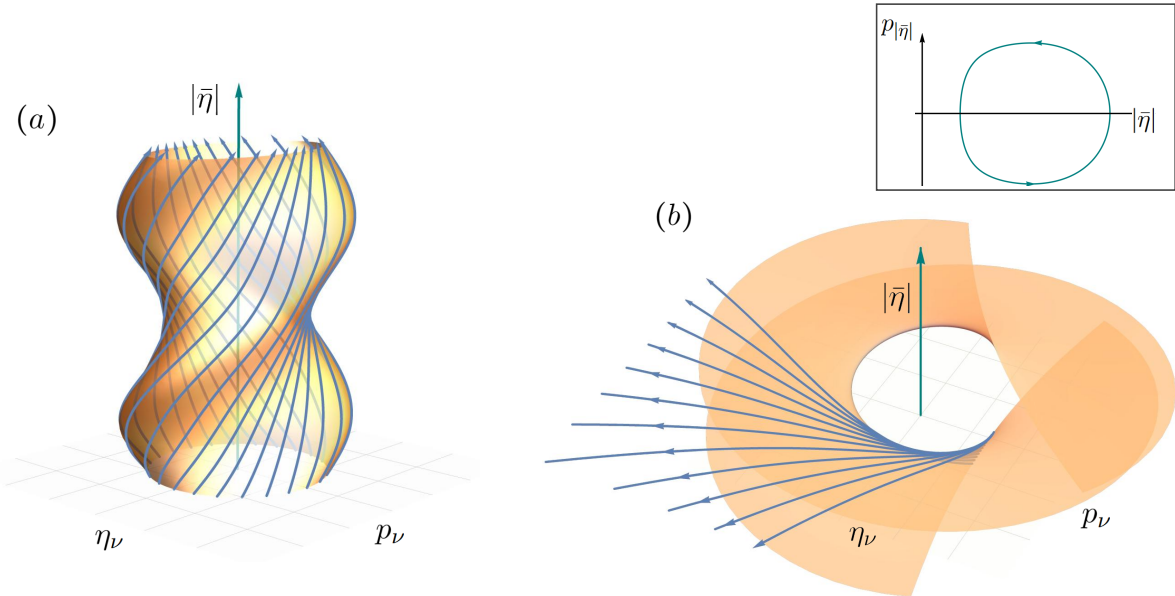


FIG. 1. Structure of the $p_\nu, \eta_\nu, |\bar{\eta}| = \xi$ section of the phase space in the linear regime $p_\nu, \eta_\nu = O(1)$ in the off-resonant (a) and resonant case (b) respectively. The presence of the integrals of motion constrains the trajectories $(p_\nu, \eta_\nu, |\bar{\eta}|)$ (blue) on the manifold $\epsilon_\nu = \text{const}$ (yellow), while the trajectory of the $(p_{|\bar{\eta}|}, |\bar{\eta}|)$ is shown in the inset. While in the off-resonant case the $|\bar{\eta}| = \text{const}$ sections of the manifolds are ellipses, preventing the indefinite growth of the η_ν, p_ν ; if a resonance occurs η_ν, p_ν are no longer bounded as these sections are hyperbolas.

First, as already noticed in Ref. [65], in addition to \mathcal{H} itself, the dynamics is constrained by the presence of N trivial integrals of motions, namely $\ell_k = \Im(\eta_k^* p_k)$ linked to the global $U(1)$ symmetry of the Hamiltonian. These are the classical angular momenta. As the number of (real) degrees of freedom is $2N$, this is not enough to make the system integrable.

On the other hand, like the spherical counterpart of Hamiltonian (18), introduced by C. Neumann [66–68], Hamiltonian (7) is known to actually admit a second set of integrals of motion [69, 70] in the form of dressed single-mode energies

$$\epsilon_\nu = \frac{1}{2} (|p_\nu^2| + (r + \omega_\nu^2)|\eta_\nu^2|) + \frac{\lambda}{4N} |\eta_\nu^2| \sum_\mu |\eta_\mu^2| + \frac{\lambda}{4N} \sum_{\mu \neq \nu} \frac{|p_\nu^2 \eta_\nu^2| + |p_\nu^2 \eta_\mu^2| - 2\Re(\eta_\nu^* p_\nu) \Re(\eta_\mu^* p_\mu)}{\omega_\mu^2 - \omega_\nu^2}, \quad (19)$$

which are analogous to the so-called Uhlenbeck integrals for the Neumann model [68]. Recently this formalism has been applied to the study of the classical dynamics of the disordered model [71–74]. Notice that $\mathcal{H} = \sum_\nu \epsilon_\nu = N\epsilon$.

V. LINEAR REGIME

In general, the analytic solution of Eq. (17) is not available. Yet, the existence of the integrals of motions (19) allows us to derive the conditions under which a mode is resonant or not. Then, as long as η_ν , the momenta p_ν are $O(1)$ and all the integrals of motions can be rewritten as

$$\epsilon_\nu = \frac{1}{2} (p_\nu^*, \eta_\nu^*) \begin{pmatrix} U_\nu & -Q_\nu \\ -Q_\nu & T_\nu \end{pmatrix} \begin{pmatrix} p_\nu \\ \eta_\nu \end{pmatrix} \quad (20)$$

where now U_ν, T_ν, Q_ν , are functions of $\bar{\eta}$ and \bar{p} alone. The matrices read

$$U_\nu = 1 + \frac{\lambda}{2} \frac{|\bar{\eta}|^2}{1 - \omega_\nu^2}, \quad T_\nu = r + \omega_\nu^2 + \frac{\lambda}{2} \frac{|\bar{p}|^2}{1 - \omega_\nu^2} + \frac{\lambda}{2} |\bar{\eta}|^2, \quad Q_\nu = \frac{\lambda}{2} \frac{\Re(\bar{\eta}^* \bar{p})}{1 - \omega_\nu^2}. \quad (21)$$

The determinant Δ_ν of the quadratic form in Eq. (20) is also constant and only depends on the integrals of motion ℓ and ϵ :

$$\Delta_\nu = U_\nu T_\nu - Q_\nu^2 = r + \omega_\nu^2 + \frac{\lambda \epsilon}{1 - \omega_\nu^2} + \frac{\lambda^2}{4} \frac{\ell^2}{(1 - \omega_\nu^2)^2}. \quad (22)$$

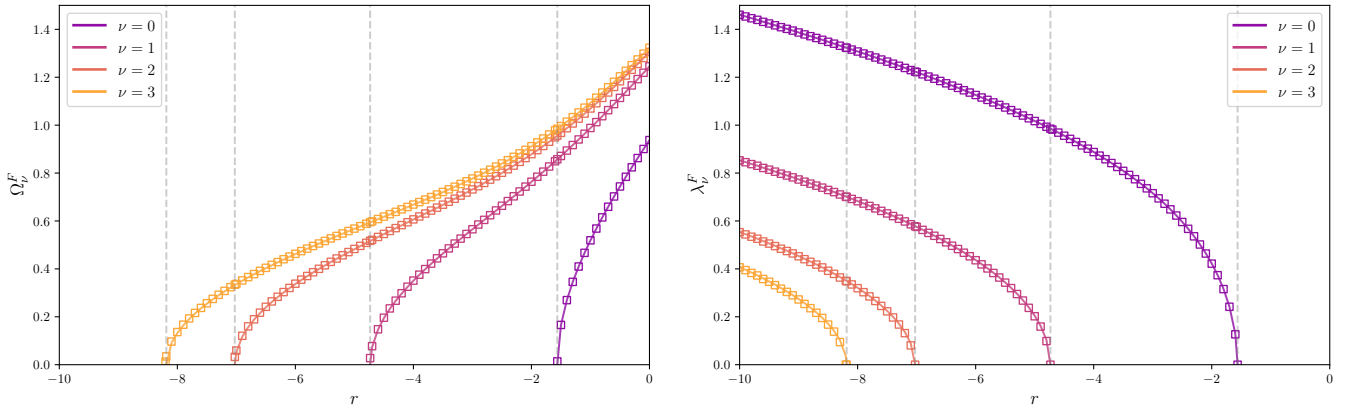


FIG. 2. Numerical estimate (diamonds) vs the theoretical estimate (Eq. (26)) of the Floquet eigenvalues λ_ν^F corresponding to the Fourier modes $\nu = 0, \dots, 3$ in the off-resonant (left) and resonant (right) regimes respectively, for a ground state quench ($m_{\text{gs}} = 6$) as a function of the final bare mass r . The vertical dotted lines represent the theoretical estimate of the boundaries r_ν^* of the resonant regions (see Eq. (33)). For the off-resonant regime ($r > r_\nu^*$, left) the Floquet frequencies are $\Omega_\nu^F = -i \lambda_\nu^F$ are shown.

Geometrically speaking, each mode is confined on a manifold that changes periodically in time with $\bar{\eta}$. The stability of this motion is thus decided by the sign of the determinant Δ_ν : positive Δ_ν corresponds to an elliptic stable manifold, while in the hyperbolic case Δ_ν resonances will occur, see Fig. 1.

In order to make this picture more quantitative, we introduce the new coordinates

$$\eta_\mu = \sqrt{U_\nu(\bar{\eta})} q_\nu \quad (23)$$

in terms of which the constant of motion take the diagonal form

$$\epsilon_\nu = \frac{1}{2} (U_\nu^2(\bar{\eta}) |\dot{q}_\nu^2| + \Delta_\nu |q_\nu^2|) . \quad (24)$$

The η_ν can be written explicitly in the linear regime as a function of the mean-field degree of freedom $\bar{\eta}$ as

$$\eta_\nu(t) = \sqrt{\frac{U_\nu(t)}{2\Delta_\nu}} \left(A_\nu^+ e^{\sqrt{-\Delta_\nu} \int_0^t dt' U_\nu^{-1}(t')} - A_\nu^- e^{-\sqrt{-\Delta_\nu} \int_0^t dt' U_\nu^{-1}(t')} \right) , \quad (25)$$

where A_ν^+ and A_ν^- are constants. As expected, the solution (25) has the form of a Bloch-Floquet wave, where

$$\lambda_\nu^F = \sqrt{-\Delta_\nu} \int_0^\tau \frac{dt}{\tau} U_\nu^{-1}(t) \quad (26)$$

are the eigenvalues of the Floquet-Hill problem, which become purely imaginary for the off-resonant case. The theoretical estimate of Eq. (26) is compared with its numerical counterpart in Fig. 2, finding excellent agreement. In particular in the off-resonant case $\Delta_\nu > 0$ ($\lambda_\nu^F = i \Omega_\nu^F$ imaginary) we have that the constants are linked to the integral of motion as

$$\frac{1}{2} (|A_\nu^+|^2 + |A_\nu^-|^2) = \epsilon_\nu \quad \frac{1}{2\sqrt{\Delta_\nu}} (|A_\nu^+|^2 - |A_\nu^-|^2) = \ell_\nu \quad (27)$$

while, if $\Delta_\nu < 0$ and the mode is resonant (λ_ν real), one has

$$\Re(A_\nu^{+*} A_\nu^-) = \epsilon_\nu, \quad \frac{1}{\sqrt{|\Delta_\nu|}} \Im(A_\nu^{+*} A_\nu^-) = \ell_\nu . \quad (28)$$

In this latter case the resonance will thus activate on a timescale $t_\nu = (2\lambda_\nu)^{-1} \ln N$, so that the period after which the system leaves the linear regime is

$$t_{\text{lin}} = \min_\nu (2\lambda_\nu)^{-1} \ln N . \quad (29)$$

Within the context of long-range physics, this can be also interpreted as the Ehrenfest timescale t_{Ehr} for which the semiclassical-mean field approximation is valid [33, 75]: in the non-resonant regime one has instead that t_{Ehr} is polynomial in N , as this is the time-scale in which the incoherent dynamics of non-resonant quantum fluctuations can affect the dynamics of macroscopic observables.

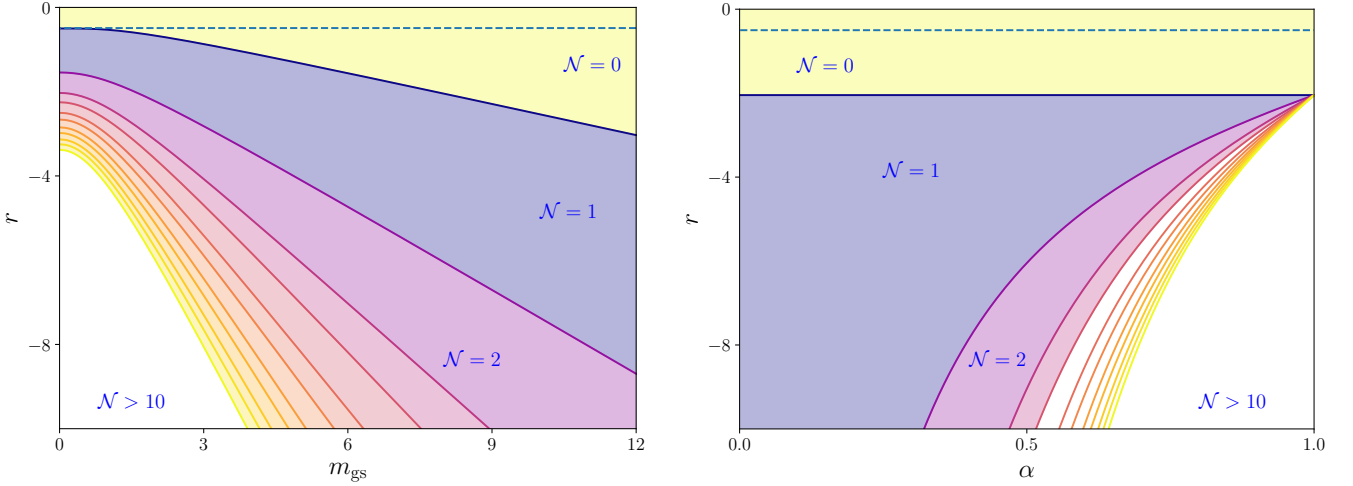


FIG. 3. Phase diagram of the number of resonances \mathcal{N} , for a ground state quench $r_- \rightarrow r$ from the massive phase as a function (left) of the ground-state mass m_{gs} and of the post-quench bare mass r for $\lambda = 1$, $\alpha = 0.5$; (right) of the range α of the interaction and of the post-quench bare mass r for $\lambda = 1$, $m_{\text{gs}} = 8$. The unbroken lines separating the boundaries corresponds to the values of r_ν^* in Eq. (33). We see that the boundary r_0^* of the off-resonant region is always below the thermal critical value r_c^{th} (dotted blue line), with $r^* \rightarrow r_c^{\text{th}}$ as $m_{\text{gs}} \rightarrow 0$. Further decreasing r more and more resonances are triggered, with the system becoming less and less stable as $m_{\text{gs}} \rightarrow 0$ and $\alpha \rightarrow 1$.

A. Stability analysis

It is instructive to take a closer look to the stability condition $\Delta_\nu > 0$, namely

$$\Delta_\nu = r + \omega_\nu^2 + \frac{\lambda\epsilon}{1 - \omega_\nu^2} + \frac{\lambda^2\ell^2}{4(1 - \omega_\nu^2)^2} > 0 \quad (30)$$

for the case of a ground-state quench. First, we notice that Δ_ν can be conveniently rewritten by introducing the turning point ξ_- of the classical dynamics of ξ , i.e. $U_{\text{eff}}(\xi_-) = \epsilon$, see Eq. (11). We have

$$\Delta_\nu = \left(1 + \frac{\lambda\xi_-^2}{2(1 - \omega_\nu^2)}\right) \left(r - r_0^* + \omega_\nu^2 + \frac{\lambda\ell^2\omega_\nu^2}{2\xi_-^2(1 - \omega_\nu^2)}\right) \quad (31)$$

where $r_0^* = -\lambda\epsilon - \frac{\lambda}{4}\ell^2$. Thus, the $\nu = 0$ mode becomes resonant for $r < r_0^*$, while further decreasing r we encounter a series of critical values r_ν^* at which the mode $\nu > 0$ activates, until the number of resonances becomes extensive as $r \rightarrow -\infty$. Integrability prevents high-energy modes from resonating before the low-energy ones, making the instability of mean-field dynamics intrinsically an infrared modes.

In particular, during a ground state quench $\ell = 1/2$ and $\xi_- = \xi(0)$, the zero mode activates at

$$r_0^* = -\frac{\lambda}{4} \left((1 + m_{\text{gs}}^2)^{1/2} + (1 + m_{\text{gs}}^2)^{-1/2} \right) \quad (32)$$

while for $\nu > 0$

$$r_\nu^* = r_0^* - \omega_\nu^2 \left(1 + \frac{\lambda}{4(1 - \omega_\nu^2)} \sqrt{1 + m_{\text{gs}}^2} \right). \quad (33)$$

Notice that $r_0^* \leq r_{\text{gs}}^c = -\frac{\lambda}{2}$, so that the quench leads to a resonant behavior only if $m^2(t = 0^+) < 0$. The phase diagram of the number of resonances \mathcal{N} of the model is shown in Fig. 3, both for fixed α and as a function of α .

If no resonance occurs ($\mathcal{N} = 0$), the correlations do not spread. If only the $\nu = 0$ mode is resonating ($\mathcal{N} = 1$), instead, long-range order appears, as a spatially constant term is generated in the correlations. Let us notice that $\mathcal{N} = 0, \mathcal{N} = 1$ phases are the only compatible with an effective permutational symmetry of the system, which is not exact at the level of the Hamiltonian for $\alpha \neq 0$, but it is restored at the dynamical level. These are the only surviving phases in the $\alpha \rightarrow 0$ limit (see Fig. 3), where the permutational symmetry becomes exact.

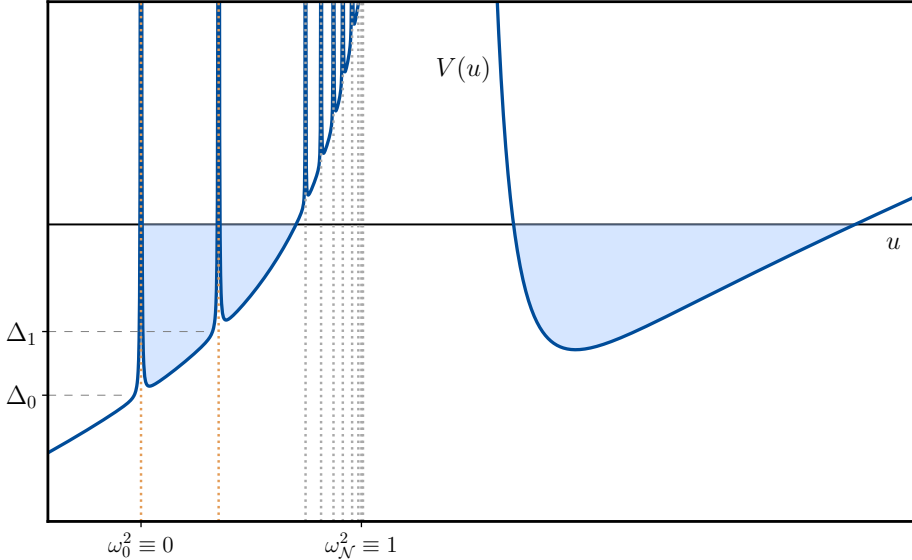


FIG. 4. Sketch of the dynamics of the Jacobi quasiparticles of the long-range $O(n)$ model in the case $\mathcal{N} = 2$. Here the dotted lines represent the dispersion ω_ν^2 of the modes, the activated ones, $\nu = 0, 1$, with $\Delta_\nu < 0$ being in yellow. Each resonant mode corresponds to a Jacobi quasiparticle, which oscillates within the corresponding accessible region, while the last quasiparticle ($u_N > \omega_N^2 \equiv 1$) corresponds instead to the classical degree of freedom. The poles corresponding to the off-resonant modes, absent from Eq. (39), are here shown to clarify their irrelevance in the thermodynamic limit.

VI. BEYOND THE LINEAR REGIME

In the resonant case, on timescales $t_{\text{Ehr}} \sim \ln N$ the linear solution breaks down. In the case one has \mathcal{N} resonances, it is convenient to redefine $p_\nu = \sqrt{N} \bar{p}_\nu$, $\eta_\nu = \sqrt{N} \bar{\eta}_\nu$, with $\nu = 0, \dots, \mathcal{N} - 1$. In this notation, it is also convenient to denote $\bar{\eta}_N \equiv \bar{\eta}, \bar{p}_N \equiv \bar{p}$, with $\omega_N = 1$. In this case we can rewrite \mathcal{H} as an effective Hamiltonian with $\mathcal{N} + 1$ degrees of freedom, namely

$$\mathcal{H}_N = \frac{1}{2} \sum_{\nu=0}^{\mathcal{N}} (|\bar{p}_\nu^2| + (r + \omega_\nu^2)|\bar{\eta}_\nu^2|) + \frac{\lambda}{4} \left(\sum_{\nu=0}^{\mathcal{N}} |\bar{\eta}_\nu^2| \right)^2 \quad (34)$$

(notice that here the parameter λ appears without the rescaling with N). On the other hand, since $\bar{p}_\nu(0), \bar{\eta}_\nu(0) = O(N^{-1/2})$, all the integral of motions ϵ_ν, ℓ_ν with $\nu = 0, \dots, \mathcal{N} - 1$ are now $O(N^{-1})$, while $\epsilon_\infty = \epsilon, \ell_\infty = \ell$. In particular, one has $\ell_\nu/N = \Im(\bar{\eta}_\nu^* \bar{p}_\nu)$ and

$$\frac{\epsilon_\nu}{N} = \frac{1}{2} (|\bar{p}_\nu^2| + (r + \omega_\nu^2)|\bar{\eta}_\nu^2|) + \frac{\lambda}{4} |\bar{\eta}_\nu^2| \sum_{\mu=0}^{\mathcal{N}} |\bar{\eta}_\mu^2| + \frac{\lambda}{4} \sum_{\mu \neq \nu}^{\mathcal{N}} \frac{|\bar{p}_\mu^2 \bar{\eta}_\nu^2| + |\bar{p}_\nu^2 \bar{\eta}_\mu^2| - 2\Re(\bar{\eta}_\mu^* \bar{p}_\mu) \Re(\bar{\eta}_\nu^* \bar{p}_\nu)}{\omega_\mu^2 - \omega_\nu^2}. \quad (35)$$

As the number of effective degrees of freedom is now reduced, it is convenient to introduce a suitable set of separable coordinates, the Jacobi elliptic coordinates [76] $u_\nu, \nu = 0, \dots, \mathcal{N}$, which are defined as the zeros of the function

$$\varphi(u) = 1 - \frac{\lambda}{2} \sum_{\nu=0}^{\mathcal{N}} \frac{|\bar{\eta}_\nu|^2}{u - \omega_\nu^2} = \prod_{\nu=0}^{\mathcal{N}} \frac{u - u_\nu}{u - \omega_\nu^2}, \quad (36)$$

and their relative momenta, which are given by

$$P_\nu = \frac{1}{2\lambda} \partial_t \varphi(u)|_{u=u_\nu} = \frac{1}{2\lambda} \frac{\dot{u}_\nu}{u_\nu - \omega_\nu^2} \prod_{\mu \neq \nu} \frac{u_\nu - u_\mu}{u_\nu - \omega_\mu^2} \quad (37)$$

see App. A for the details. Due to the form of the function $\varphi(u)$, u_ν is such that $\omega_\nu < u_\nu < \omega_{\nu+1}$ for all $\nu \neq \mathcal{N} - 1$, while u_N is confined in the semi-axis $u > \omega_N = 1$. In particular, in the case $\mathcal{N} = 1$ we recover the classical degree of

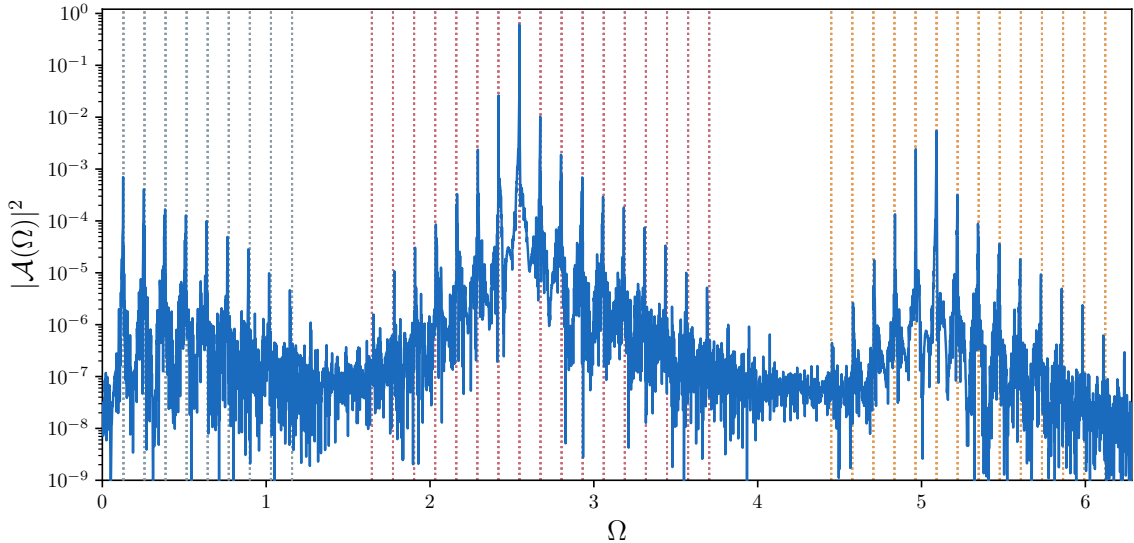


FIG. 5. Spectral density of $\mathcal{A}(t) = m^2(t) - \overline{m^2}$ (̄ representing the time average), for the single-resonance ($\mathcal{N} = 1$) phase. The location of the peaks is compared with the expected quasi-periodic comb-structure $p_0 \Omega_0 + p_1 \Omega_1$, $p_0, p_1 \in \mathbb{Z}$ (dashed vertical lines), finding an excellent agreement. Here Ω_1 , corresponding to the most prominent peak, coincides with the frequency of the classical motion in Eq. (10), while $\Omega_0 \sim (\ln N)^{-1}$ is the resonant frequency in Eq. (43). Peaks close to the different harmonics $p_1 \Omega_1$ of the classical frequency are highlighted in different colors. We considered a quench from $m_{\text{gs}} = 6$ to $r = -2$ with $\lambda = 1$, $N = 10^{14}$. Due to the logarithmic scaling in Ω_0 , such a large value of N is needed both to have a clear scale separation and to get rid of finite-size effects.

freedom as $u_1(t) = 1 + \lambda \xi^2(t)/2$. As shown in the App. A, see also Refs. [62, 70], the set u_ν , P_ν is indeed separable, as

$$\lambda^2 P_\nu^2 + V(u_\nu) = 0 \quad (38)$$

where $V(u)$ is the potential

$$V(u) = u + r - \frac{\lambda}{N} \sum_{\nu=0}^{\mathcal{N}} \frac{\epsilon_\nu}{u - \omega_\nu^2} + \frac{\lambda^2}{4N} \sum_{\nu=0}^{\mathcal{N}} \frac{\ell_\nu^2}{(u - \omega_\nu^2)^2}. \quad (39)$$

Since the motion takes place within the regions $V(u) < 0$ ($u > 0$) the inversion points u_ν^\pm of each u_ν coincide with the positive zeros of $V(u)$. Thus, the energy of the quasi-particles u_ν oscillates between the inversion points u_ν^\pm (see Fig. 4).

A. Spectrum of the resonances

As the system is integrable also beyond the linear regime, the dynamics of the resonant modes can be written as the superposition of \mathcal{N} frequencies $\{\Omega_\nu\}$. Of these $\mathcal{N} - 1$ are of order $(\ln N)^{-1}$, as they correspond to the resonances, while the last one will correspond to the classical mean-field frequency.

However, these frequencies do not correspond to the ones of a particle in the potential $V(u)$ as $P_\nu \neq \dot{u}_\nu$, and the u_ν will not be periodic. Instead, the frequencies can be computed by expressing $\mathcal{H}_\mathcal{N}$ in terms of the action variables

$$J_\nu = \oint \frac{du_\nu}{2\pi} P_\nu = \int_{u_\nu^-}^{u_\nu^+} \frac{du}{\pi\lambda} \sqrt{-V(u)}. \quad (40)$$

and by computing $\Omega_\nu = \partial\mathcal{H}/\partial J_\nu$.

From Eq. (39) it follows that, close to the poles of $V(u)$ one has

$$V(u) = \frac{\lambda^2 \ell_\nu^2}{4N^2(u - \omega_\nu^2)^2} - \frac{\lambda \epsilon_\nu}{N(u - \omega_\nu^2)} + \Delta_\nu \quad (41)$$

where Δ_ν is the same stability parameter defined in Eq. (22). As shown in Fig. 4, the resonant modes with $\Delta_\nu < 0$ correspond to finite amplitude oscillations, while off-resonant frequencies result in oscillations with vanishing amplitude, whose effect is negligible at large N . Instead, the inversion points u_ν^\pm of the resonant modes $\nu = 0, \dots, \mathcal{N} - 1$ will approach ω_ν^2 and $\omega_{\nu+1}^2$ respectively in the thermodynamic limit. As shown in App. B, at the leading order in N one has

$$\mathcal{H}_{\mathcal{N}} = \bar{H}(J_{\mathcal{N}}) + \frac{2\pi}{\ln N} \sum_{\nu=0}^{\mathcal{N}-1} J_\nu \sum_{\mu=0}^{\nu} \sqrt{|\Delta_\mu|} \quad (42)$$

where $\bar{H}(J_{\mathcal{N}})$ corresponds to the Hamiltonian of the classical degree of freedom. Finally, for the resonant modes $\nu = 0, \dots, \mathcal{N} - 1$, one can write

$$\Omega_\nu = \frac{2\pi}{\ln N} \sum_{\mu=0}^{\nu} \sqrt{|\Delta_\mu|}. \quad (43)$$

As expected, we find a quasi-periodic motion in which the frequency $\Omega_{\mathcal{N}} = O(1)$ of the classical-mean field motion, see Eq. (10) coexists with the resonant frequencies $\Omega_\nu \sim (\ln N)^{-1}$, $\nu = 0, \dots, \mathcal{N} - 1$. This prediction has been compared with the numerics for the single resonance case $\mathcal{N} = 1$ in Fig. 5 where the spectral density of the observable $m^2(t)$ is analyzed. This case corresponds to an unbroken effective permutational symmetry. Thus, a clear scale separation is observed, as the dynamics is the superposition of two different frequencies and the classical motion can be seen as a fast beat on top of the slow resonant dynamics. The resonant mode $|\bar{\eta}_0|$ will periodically return small, with a period $\Omega_0^{-1} \sim \ln N$.

VII. CORRELATIONS AND ENTANGLEMENT SPREADING

As the mean-field degree of freedom $\bar{\eta}$ is linked to one-site dynamics, we expect quantum correlation between different sites only to arise due to resonances. This expectation is indeed confirmed by the analysis of Ref. [55]. In this section, we revise the link between entanglement spreading and the presence of resonances and derive semi-analytical expression for the entanglement spreading. The presence of resonances thus gradually drives the system away from the mean field description, which is completely washed away in the limit of an extensive $\mathcal{N} \sim N$.

As a measure of the quantum spatial correlations we will consider the entanglement entropy S associated with a bipartition of the system into an interval A of length L_A and its complement. It is defined as $S = -\text{tr} \rho_A \ln \rho_A$, where $\rho_A = \text{tr}_{\bar{A}} \rho$ is the reduced density matrix associated with the subsystem A . In the case of periodic boundary conditions, the exact position of the interval is not relevant. The entropy $S(t)$ can be in turn expressed in terms of the two-point correlations of the bosonic operators Φ_j , Π_j ,

$$\gamma = \text{Re} \begin{pmatrix} \langle \Phi_j(t) \Phi_{j'}(t) \rangle & \langle \Phi_j(t) \Pi_{j'}(t) \rangle \\ \langle \Pi_j(t) \Phi_{j'}(t) \rangle & \langle \Pi_j(t) \Pi_{j'}(t) \rangle \end{pmatrix} \quad (44)$$

by following the procedure of Ref. [77]. This is a consequence of two facts: (i) for a ground state quench the initial state $\rho(0)$ is a bosonic Gaussian state, (ii) in the $n \rightarrow \infty$ limit, the state of system remains Gaussian at any time t . In particular, we have $S(t) = \sum_n s(\sigma_n)$ where

$$s(\sigma) = \left(\sigma + \frac{1}{2} \right) \ln \left(\sigma + \frac{1}{2} \right) - \left(\sigma - \frac{1}{2} \right) \ln \left(\sigma - \frac{1}{2} \right), \quad (45)$$

and σ_n are the symplectic eigenvalues of the matrix γ in Eq. (44), reduced on the subsystem $j, j' \in A$. More explicitly, if we denote such a reduced correlation matrix as γ_{red} , the σ_n are a set of L_A positive numbers which are eigenvalues of $i\mathbb{J}\gamma_{\text{red}}$, \mathbb{J} being the symplectic identity

$$\mathbb{J} = \begin{pmatrix} 0 & \mathbb{I}_L \\ -\mathbb{I}_L & 0 \end{pmatrix}. \quad (46)$$

In the limit of large size N , the matrix γ_{red} will be dominated by the classical mode $\bar{\eta}$ and the resonant ones, as the

latter becomes $O(\sqrt{N})$ on $t \sim \ln N$. More explicitly

$$\begin{aligned} \langle \Phi_j \Phi_{j'} \rangle &= |\bar{\eta}^2| \delta_{j'j} + \sum_{\nu=0}^{\mathcal{N}-1} (|\bar{\eta}_\nu^2| - N^{-1}|\bar{\eta}^2|) e^{2\pi i \nu(j-j')/N}, \quad \langle \Pi_j \Pi_{j'} \rangle = |\bar{p}^2| \delta_{j'j} + \sum_{\nu=0}^{\mathcal{N}-1} (|\bar{p}_\nu^2| - N^{-1}|\bar{p}^2|) e^{2\pi i \nu(j-j')/N}, \\ \Re \langle \Pi_j \Phi_{j'} \rangle &= \Re(\bar{p}^* \bar{\eta}) \delta_{j'j} + \sum_{\nu=0}^{\mathcal{N}-1} (\Re(\bar{p}_\nu^* \bar{\eta}_\nu) - N^{-1} \Re(\bar{p}^* \bar{\eta})) e^{2\pi i \nu(x-x')/N}. \end{aligned} \quad (47)$$

Different regimes appear

- *Case $\mathcal{N} = 0$:* in this case the correlations in Eqs. (47) are all diagonal and $\sigma_n^2 = |\bar{\eta}|^2 |\bar{p}|^2 - \Re(\bar{p}^* \bar{\eta})^2 = \Im(\bar{p}^* \bar{\eta}) = \ell^2$, so that has $\sigma_n = \ell$ for any $n = 1, \dots, L_A$. As $S(t)$ remains constant, no entanglement is generated. Since for a ground state quench $\ell = 1/2$, $S(t) \equiv 0$ as expected from Eq. (45).
- *Case $\mathcal{N} = 1$:* in this case we have $\langle \Phi_j \Phi_{j'} \rangle = |\bar{\eta}^2| \delta_{j'j} + |\bar{\eta}_0^2| - N^{-1} |\bar{\eta}^2|$ (and analogously for the momentum and cross correlations). Only for $n = 1$, $\sigma_n \neq 1/2$ and the entanglement contribution is given by

$$\sigma_1 = \frac{1}{2} \sqrt{1 - 2\rho(1-\rho) + 4L_A(1-\rho)\chi(t)} \quad (48)$$

where $\rho = L_A/N$ and

$$\chi_1(t) = |\bar{p}_0^2 \bar{\eta}_1^2| + |\bar{p}_1^2 \bar{\eta}_0^2| - 2\Re(\bar{p}_1^* \bar{\eta}_1) \Re(\bar{p}_0^* \bar{\eta}_0) \quad (49)$$

represents the overlap between the resonant mode $\bar{\eta}_0$ and the classical one $\bar{\eta}_1 \equiv \bar{\eta}$. Here, $S(t) \approx 0$ at any time when $\bar{\eta}_0$ is small, so that quantum correlations follow a quasi-periodic pattern, on a timescale $\sim \ln N$. When the resonance is active $\chi_1(t) = O(1)$, and $\sigma_1 = O(L^{1/2})$. In particular, for $L_A \gg 1$ we find

$$S(t) \sim \frac{1}{2} \ln L_A(1-\rho) \chi_1(t) \quad (50)$$

so that the maximum entangled generated is order $1/2 \ln L_A$, as observed also for long-range spin systems [75].

- *Case $\mathcal{N} > 1$:* the permutational symmetry is effectively broken and the correlations acquire a spatial modulation, making an explicit computation of $S(t)$ impossible. However, close expressions can be derived in the regime $L_A \gg 1$. Indeed, while the spatial modulation of the modes can no longer be ignored for $L_A = O(N)$, a principal component analysis of the L_A by L_A correlation matrix γ_{red} reveals that only a number $\lfloor \mathcal{N}/2 \rfloor$ of $O(L)$ eigenvalues σ_n actually contributes to the entropy. In particular, as shown in App. C, we have

$$S(t) \sim \frac{1}{2} \ln \text{pdet } \Gamma(t) \quad (51)$$

where pdet denotes the pseudo-determinant of the \mathcal{N} by \mathcal{N} , skew symmetric matrix

$$\Gamma_{\mu\nu} = N \frac{\sin \pi \rho(\mu - \nu)}{\pi(\mu - \nu)} (\bar{\eta}_\mu \bar{p}_\nu - \bar{\eta}_\nu \bar{p}_\mu). \quad (52)$$

In particular, for $\mathcal{N} = 2$ one has

$$S(t) \sim \ln L_A (\bar{\eta}_1 \bar{p}_2 - \bar{\eta}_2 \bar{p}_1) \text{sinc}(\pi \rho) \quad (53)$$

while for $\mathcal{N} = 3$

$$S(t) \sim \frac{1}{2} \ln L_A^2 \sum_{\mu>\nu}^2 (\bar{\eta}_\mu \bar{p}_\nu - \bar{\eta}_\nu \bar{p}_\mu)^2 \text{sinc}^2(\pi(\mu - \nu)\rho). \quad (54)$$

Finally, in the regime $1 \ll L_A \ll N$ our analysis reveals the trend

$$S(t) \sim \frac{1}{2} \ln L_A^2 \sum_{\mu>\nu}^{\mathcal{N}-1} (\bar{\eta}_\mu \bar{p}_\nu - \bar{\eta}_\nu \bar{p}_\mu)^2 \quad (55)$$

valid for all $\mathcal{N} > 1$. Notice that, as now the dynamics of the resonant mode is given by the interference of different frequencies, $S(t)$ oscillates around a finite value, as a finite amount of entanglement is generated. Moreover, let us notice that in this case the maximum amount of entanglement generated is of order $S(t) \sim \ln L_A$.

In summary, quantum resonances are the mechanism that spreads correlations in strong long-range systems, disrupting the mean-field dynamics. Since $S \sim c \ln L_A$, entanglement never obeys volume-law as in the short-range limit, in line with the general understanding of strong long-range dynamics [55, 60, 75]. In addition, our analysis reveals the importance of the multi-resonant regime: the presence of spatially-modulated resonances ($\mathcal{N} \geq 2$) results in an enhanced entanglement production ($c = 1$ versus $c = 1/2$ of the single resonance case). Multi-resonances are also associated with a stable production of entanglement due to the interference among different resonant modes.

VIII. CONCLUSIONS

In this work, we developed a comprehensive and quantitative framework for the far-from-equilibrium dynamics of the strong long-range quantum $O(n)$ model in the large- n limit, expanding the previous results of [55] and generalizing the recent results of [62] about the integrability of the large- n dynamics. This allowed us to understand the interplay between classical ultra-local degrees of freedom and the quantum modes, responsible of the rich dynamics observed on mesoscopic timescales $t_{\text{Ehr}} \sim \ln N$. The key mechanism enabling this complexity is the onset of a finite number \mathcal{N} of parametric resonances in the quantum modes, triggered by the discrete nature of the long-range dispersion.

In particular, the knowledge of the whole set of the integrals of motion allows to determine the resonance condition and the associated phase diagram, to construct a reduced Hamiltonian governing the resonant sector and to derive the associated spectrum of the model. This approach also provides a unified interpretation of finite-size effects, revealing how strong-long-range systems deviates gradually from mean-field behavior as the number of resonant modes \mathcal{N} increases: in particular, while in the strict thermodynamic limit, $N \rightarrow \infty$, an effective invariance under permutations is recovered, the presence of multiple resonances can destroy it within the time-scale t_{Ehr} . The resonant sector is also responsible for the spreading of quantum correlations, quantified here by the entanglement entropy $S(t)$. While the quasi-mean field nature prevents the onset of volume-law phases, the presence of multiple resonant modes \mathcal{N} enhances both the rate and the stability of entanglement production.

The present framework highlights the role of the $O(n)$ model as a paradigmatic setting for understanding quantum dynamics, both in the short-range and long-range regimes, placing the present work within the long line of studies that have used the large- n as benchmark for critical phenomena, quench dynamics [25, 51, 54, 65, 78]. At the same time, the results obtained here also contribute to the broader ongoing program aimed at characterizing the dynamics of quantum systems in the presence of long-range interactions: within this context the exact solution of the $O(n)$ model brings a deeper understanding of this class of model and can constitute an ideal starting point for several generalizations and approximations, e.g. the $1/n$ expansion [24].

Our analysis can be extended to the long-range-to-short-range crossover, understanding how the resonance mechanism and the time-scale separation break down as the decay exponent approaches the weak-long-range regime, $\alpha \rightarrow d$. In particular, it would be interesting to investigate the relation among the classical oscillations of the high-energy ultra-local mode and the undamped oscillations observed in the short-range regime of the $O(n)$ model [54], which have recently been related to the presence of high-energy Higgs oscillations coming from beyond the edge of the spectral band [62].

Finally, the present framework could be expanded to explain the interplay between persistent mean-field oscillations and spatially-modulated quantum modes observed in other strong-long-range models—most notably in semiclassical analyses of the LMG model [56] (see e.g. Refs. [57, 60]). As the interplay between semiclassical chaos and emergent integrability in long-range many-body systems remains largely unexplored, clarifying whether such oscillations can be universally interpreted as manifestations of resonant or near-integrable sectors would significantly unify the phenomenology of long-range models.

IX. ACKNOWLEDGMENT

GG acknowledges the support of the MSCA Grant 101152898 (DREAMS). This research was funded by the Swiss National Science Foundation (SNSF) grant numbers 200021–207537 and 200021–236722, by the Deutsche Forschungsgemeinschaft (DFG, German Research Foundation) under Germany’s Excellence Strategy EXC2181/1-390900948 (the Heidelberg STRUCTURES Excellence Cluster) and by the European Union under GA No. 101077500–QLRNet. Partial support by grant NSF PHY-230935 to the Kavli Institute for Theoretical Physics (KITP) is also acknowledged.

Appendix A: Separability of the Jacobi coordinates

Let us set $\eta_\nu = \xi_\nu e^{i\theta_\nu}$: as θ_ν is cyclic, one has that θ_ν, ℓ_ν are trivially a pair of separable canonical coordinates. The Jacobi coordinates can be thought as a point canonical transformation from the ξ_ν to the u_ν , defined as

$$\varphi(u) = 1 - \frac{\lambda}{2N} \sum_\nu \frac{\xi_\nu^2}{u - \omega_\nu^2} = \prod_\nu \frac{u - u_\nu}{u - \omega_\nu}. \quad (\text{A1})$$

We will now prove that the u_ν are a set of separable coordinates for \mathcal{H}_N in (34).

First we notice that, by replacing the equations of motion in $\partial_t^2 \phi$ and by making use of the elementary identity

$$\frac{1}{(u - u_\nu)(u - u_\mu)} = \frac{1}{u_\nu - u_\mu} \left(\frac{1}{u - u_\nu} - \frac{1}{u - u_\mu} \right) \quad (\text{A2})$$

(with $\nu \neq \mu$) we find

$$V(u) = (u + m^2)\varphi^2 + \frac{1}{2}\varphi \partial_t^2 \varphi(u) - \frac{1}{4}(\partial_t \varphi)^2, \quad (\text{A3})$$

which for $u = u_\nu$ becomes

$$V(u_\nu) + \frac{1}{4}(\partial_t \varphi)^2|_{u=u_\nu} = 0. \quad (\text{A4})$$

To prove Eq. (38), and thus the separability of the set $\{u_\nu\}$ one has to show that the momentum conjugate to u_ν is $P_\nu = (2\lambda)^{-1} \partial_t \varphi|_{u=u_\nu}$.

The momentum P_ν conjugate to u_ν is defined as

$$P_\nu = \sum_\mu \frac{\partial \xi_\mu}{\partial u_\nu} p_\mu \quad (\text{A5})$$

It is thus convenient to write explicitly the ξ_ν in terms of the u_ν , which can be done by as the ξ_ν are linked to the residues of the poles of $\varphi(u)$. We get

$$\frac{\lambda}{4} \xi_\nu^2 = (\omega_\nu^2 - u_\nu) \prod_{\omega_\nu \neq \omega_\mu} \frac{\omega_\nu^2 - u_\mu}{\omega_\nu^2 - \omega_\mu^2}, \quad (\text{A6})$$

from which

$$\frac{1}{\xi_\nu} \frac{\partial \xi_\nu}{\partial u_\mu} = \frac{1}{2} \frac{1}{\omega_\nu^2 - u_\mu}, \quad (\text{A7})$$

and finally

$$P_\nu = \sum_\mu \frac{\partial \xi_\mu}{\partial u_\nu} p_\mu = \frac{1}{2} \sum_\mu \frac{\xi_\mu p_\mu}{\omega_\mu^2 - u_\nu} = -\frac{1}{2\lambda} \partial_t \varphi|_{u=u_\nu}, \quad (\text{A8})$$

where we used the equation of motion $\dot{\xi}_\nu = p_\nu$ for the original variables. This proves the separability.

Let us notice that, more explicitly, one has

$$P_\nu = \frac{N}{2\lambda} \frac{\dot{u}_\nu}{u_\nu - \omega_\mu^2} \prod_{\nu \neq \mu} \frac{u_\nu - u_\mu}{u_\nu - \omega_\mu^2}. \quad (\text{A9})$$

Appendix B: Computation of the action variables

We want now to compute the action variables J_ν in Eq. (40). Let us first notice that, far from the poles $u = \omega_\nu^2$ of the potential $V(u)$, in the limit $N \rightarrow \infty$ we have

$$V(u) \approx \tilde{V}(u) = u + r - \frac{\lambda \epsilon_N}{u - 1} + \frac{\lambda^2 \ell_N^2}{4(u - 1)^2} \quad (\text{B1})$$

up to $O(N^{-1})$, while close to the poles

$$V(u) \approx \Delta_\nu - \frac{\lambda\epsilon_\nu}{N(u - \omega_\nu^2)} + \frac{\lambda^2\ell_\nu^2}{4N^2(u - \omega_\nu^2)^2}. \quad (\text{B2})$$

On the other hand, in this limit $u_\nu^- = \omega_\nu^2 + O(N^{-1})$, $u_\nu^+ = \omega_{\nu+1}^2 + O(N^{-1})$ for $\nu = 0, \dots, \mathcal{N} - 1$, so that we have

$$J_\nu = \int_{\omega_\nu^2}^{\omega_{\nu+1}^2} \frac{du}{\pi\lambda} \sqrt{-\tilde{V}(u)} + \frac{\ln N}{2\pi N} \left(\frac{\epsilon_\nu}{\sqrt{|\Delta_\nu|}} - \frac{\epsilon_{\nu+1}}{\sqrt{|\Delta_{\nu+1}|}} \right) + O(N^{-1}) \quad (\text{B3})$$

for $\nu = 0, \dots, \mathcal{N} - 2$ while

$$J_{\mathcal{N}-1} = \int_{\omega_\nu^2}^{u_{\mathcal{N}-1}^+} \frac{du}{\pi\lambda} \sqrt{-\tilde{V}(u)} + \frac{\ln N}{2\pi N} \frac{\epsilon_{\mathcal{N}-1}}{\sqrt{|\Delta_{\mathcal{N}-1}|}} + O(N^{-1}) \quad (\text{B4})$$

and

$$J_{\mathcal{N}} = \int_{u_{\mathcal{N}}^-}^{u_{\mathcal{N}}^+} \frac{du}{\pi\lambda} \sqrt{-\tilde{V}(u)} + O(N^{-1}). \quad (\text{B5})$$

We have that

$$\sum_{\mu=\nu}^{\mathcal{N}-1} J_\mu = \int_{\omega_\nu^2}^{u_{\mathcal{N}-1}^+} \frac{du}{\pi\lambda} \sqrt{-\tilde{V}(u)} + \frac{\ln N}{2\pi N} \frac{\epsilon_\nu}{\sqrt{|\Delta_\nu|}} + O(N^{-1}) \quad (\text{B6})$$

Let us notice that $\tilde{V}(u)$ depends only on $\epsilon_{\mathcal{N}}$: we have then that

$$J_{\mathcal{N}} = f_{\mathcal{N}}(\epsilon_{\mathcal{N}}) \quad (\text{B7})$$

while for $\nu = 0, \dots, \mathcal{N} - 1$

$$\frac{\epsilon_\nu}{N} = \frac{2\pi\sqrt{|\Delta_\nu|}}{\ln N} \left(-f_\nu(\epsilon_{\mathcal{N}}) + \sum_{\mu=\nu}^{\mathcal{N}-1} J_\mu + O(N^{-1}) \right) \quad (\text{B8})$$

(where f_ν are a set of function implicitly defined by the above expressions). Finally one has

$$\mathcal{H}_{\mathcal{N}} = \epsilon_{\mathcal{N}} + \frac{1}{N} \sum_{\mu=0}^{N-1} \epsilon_\mu = \bar{H}(J_{\mathcal{N}}) + \frac{2\pi}{\ln N} \sum_{\nu=0}^{\mathcal{N}-1} J_\nu \sum_{\mu=0}^{\nu} \sqrt{|\Delta_\mu|} + o(N^{-1}) \quad (\text{B9})$$

where at the leading order in N , \bar{H} is the Hamiltonian of the collective mode $\bar{\eta}$.

Appendix C: Entanglement entropy for the multi-resonant case

We want now to prove Eq. (51) for $S(t)$ in the multi-resonant case. In this case, the leading contribution to $S(t)$ comes from the overlap between resonances, so that we can neglect the contribution of the classical, mean-field mode $\bar{\eta}$. More formally, we define the

$$\langle j | \nu \rangle = \frac{1}{\sqrt{N}} e^{2\pi i \nu \cdot j / N} \quad (\text{C1})$$

with $j \in \{1, L\}$, $\nu \in \{0, \mathcal{N} - 1\}$, corresponding to the spatial modulation of the resonances. While the vectors are orthogonal on the whole system, on the subspace A one has a finite overlap between resonances given by

$$\langle \mu | \nu \rangle = \frac{\sin(\pi\rho(\mu - \nu))}{\pi(\mu - \nu)}, \quad (\text{C2})$$

where once again $\rho = L_A/N$. Finally as $\Im(\bar{p}_\nu^* \bar{\eta}_\nu) = O(N^{-1})$, we choose $\bar{\eta}_\nu, \bar{\eta}_\mu$ to be real. One has thus

$$\gamma_{\text{red}} = N \begin{pmatrix} Q & R \\ R & P \end{pmatrix}, \quad (\text{C3})$$

with

$$Q = \sum_{\nu=0}^{\mathcal{N}-1} \bar{\eta}_\nu^2 |\nu\rangle \langle \nu|, \quad P = \sum_{\nu=0}^{\mathcal{N}-1} \bar{p}_\nu^2 |\nu\rangle \langle \nu|, \quad R = \sum_{\nu=0}^{\mathcal{N}-1} \bar{p}_\nu \bar{\eta}_\nu |\nu\rangle \langle \nu|, \quad (\text{C4})$$

so that

$$i\mathbb{J}\gamma_{\text{red}} = iN \sum_{\nu} (\bar{p}_\nu |\nu\rangle_1 + \bar{\eta}_\nu |\nu\rangle_2) (-\bar{\eta}_\nu \langle \nu|_1 + \bar{p}_\nu \langle \nu|_2) \equiv iN \sum_{\nu} |u_\nu\rangle \langle v_\nu| \quad (\text{C5})$$

where $|\nu\rangle_{1,2}$ represents the vector basis acting on the two subspaces and $|u_\nu\rangle = \bar{p}_\nu |\nu\rangle_1 + \bar{\eta}_\nu |\nu\rangle_2$, $|v_\nu\rangle = -\bar{\eta}_\nu |\nu\rangle_1 + \bar{p}_\nu |\nu\rangle_2$. As the rank of $\sum_{\nu} |u_\nu\rangle \langle v_\nu|$ is at most \mathcal{N} , we will have several null eigenvalues: within our approximation, these must be interpreted as $O(N^{-1})$ eigenvalues, which in turn corresponds to the $O(1)$ σ_j , which give a subleading contribution to $S(t)$. We will just focus then on the $O(N)$ eigenvalues coming from the non-zero eigenvalues: these will coincide with the eigenvalues of the \mathcal{N} by \mathcal{N} imaginary skew-symmetric matrix

$$i\Gamma_{\mu\nu} = N \langle u_\mu | v_\nu \rangle = N(\bar{\eta}_\mu \bar{p}_\nu - \bar{\eta}_\nu \bar{p}_\mu) |\langle \mu | \nu \rangle|^2, \quad (\text{C6})$$

which correspond to Eq. (52). The spectrum of $\Gamma_{\mu\nu}$ is given by $\lfloor \mathcal{N}/2 \rfloor$ pairs $\{i\sigma_\nu, -i\sigma_\nu\}$ (with $\sigma_\nu > 0$) plus an isolated zero eigenvalue for odd \mathcal{N} . We have thus that

$$S(t) = \sum_{\nu} s(\sigma_\nu) \approx \sum_{\nu} \ln \sigma_\nu = \frac{1}{2} \ln \text{pdet}\Gamma(t) \quad (\text{C7})$$

where the pseudo-determinant pdet is the product of all the non-zero eigenvalues.

[1] A. Campa, T. Dauxois, D. Fanelli, and S. Ruffo, *Physics of Long-Range Interacting Systems* (Oxford Univ. Press, 2014).

[2] N. Defenu, T. Donner, T. Macrì, G. Pagano, S. Ruffo, and A. Trombettoni, Long-range interacting quantum systems, *Rev. Mod. Phys.* **95**, 035002 (2023).

[3] N. Defenu, A. Leroze, and S. Pappalardi, Out-of-equilibrium dynamics of quantum many-body systems with long-range interactions, *Phys. Rep.* **1074**, 1 (2024).

[4] H. Haffner, C. Ross, and R. Blatt, Quantum computing with trapped ions, *Phys. Rep.* **469**, 155–203 (2008).

[5] T. Lahaye, C. Menotti, L. Santos, M. Lewenstein, and T. Pfau, The physics of dipolar bosonic quantum gases, *Rep. Prog. Phys.* **72**, 126401 (2009).

[6] M. Saffman, T. G. Walker, and K. Mølmer, Quantum information with rydberg atoms, *Rev. Mod. Phys.* **82**, 2313 (2010).

[7] H. Ritsch, P. Domokos, F. Brennecke, and T. Esslinger, Cold atoms in cavity-generated dynamical optical potentials, *Rev. Mod. Phys.* **85**, 553 (2013).

[8] H. Bernien, S. Schwartz, A. Keesling, H. Levine, A. Omran, H. Pichler, S. Choi, A. S. Zibrov, M. Endres, M. Greiner, V. Vuletić, and M. D. Lukin, Probing many-body dynamics on a 51-atom quantum simulator, *Nature* **551**, 579 (2017).

[9] C. Monroe, W. C. Campbell, L.-M. Duan, Z.-X. Gong, A. V. Gorshkov, P. W. Hess, R. Islam, K. Kim, N. M. Linke, G. Pagano, P. Richerme, C. Senko, and N. Y. Yao, Programmable quantum simulations of spin systems with trapped ions, *Rev. Mod. Phys.* **93**, 025001 (2021).

[10] F. Mivehvar, F. Piazza, T. Donner, and H. Ritsch, Cavity QED with quantum gases: new paradigms in many-body physics, *Adv. Phys.* **70**, 1–153 (2021).

[11] J. Zhang, P. W. Hess, A. Kyprianidis, P. Becker, A. Lee, J. Smith, G. Pagano, I.-D. Potirniche, A. C. Potter, A. Vishwanath, *et al.*, Observation of a discrete time crystal, *Nature* **543**, 217 (2017).

[12] K. Baumann, C. Guerlin, F. Brennecke, and T. Esslinger, Dicke quantum phase transition with a superfluid gas in an optical cavity, *Nature* **464**, 1301 (2010).

[13] J. Rovny, R. L. Blum, and S. E. Barrett, Observation of discrete-time-crystal signatures in an ordered dipolar many-body system, *Phys. Rev. Lett.* **120**, 180603 (2018).

[14] S. Choi, J. Choi, R. Landig, G. Kucsko, H. Zhou, J. Isoya, F. Jelezko, S. Onoda, H. Sumiya, V. Khemani, *et al.*, Observation of discrete time-crystalline order in a disordered dipolar many-body system, *Nature* **543**, 221 (2017).

[15] A. Safavi-Naini, R. Lewis-Swan, J. G. Bohnet, M. Gärttner, K. Gilmore, J. Jordan, J. Cohn, J. K. Freericks, A. M. Rey, and J. Bollinger, Verification of a many-ion simulator of the Dicke model through slow quenches across a phase transition, *Phys. Rev. Lett.* **121**, 040503 (2018).

[16] A. Keesling, A. Omran, H. Levine, H. Bernien, H. Pichler, S. Choi, R. Samajdar, S. Schwartz, P. Silvi, S. Sachdev, *et al.*, Quantum Kibble–Zurek mechanism and critical dynamics on a programmable rydberg simulator, *Nature* **568**, 207 (2019).

[17] M. Kastner, Diverging equilibration times in long-range quantum spin models, *Phys. Rev. Lett.* **106**, 130601 (2011).

[18] S. Schütz and G. Morigi, Prethermalization of atoms due to photon-mediated long-range interactions, *Phys. Rev. Lett.* **113**, 203002 (2014).

[19] N. Defenu, Metastability and discrete spectrum of long-range systems, *Proceedings of the National Academy of Sciences* **118**, e2101785118 (2021).

[20] A. Pizzi, J. Knolle, and A. Nunnenkamp, Higher-order and fractional discrete time crystals in clean long-range interacting systems, *Nature communications* **12**, 2341 (2021).

[21] M. Collura, A. De Luca, D. Rossini, and A. Lerose, Discrete time-crystalline response stabilized by domain-wall confinement, *Physical Review X* **12**, 031037 (2022).

[22] G. Giachetti, A. Solfanelli, L. Correale, and N. Defenu, Fractal nature of high-order time crystal phases, *Phys. Rev. B* **108**, L140102 (2023).

[23] P. C. Hohenberg and B. I. Halperin, Theory of dynamic critical phenomena, *Reviews of Modern Physics* **49**, 435 (1977).

[24] J. Zinn-Justin, 4th ed. (Oxford University Press, Oxford, 2002).

[25] S. Sotiriadis and J. Cardy, Quantum quench in interacting field theory: A self-consistent approximation, *Phys. Rev. B* **81**, 134305 (2010).

[26] M. Uhlmann, R. Schützhold, and U. R. Fischer, System size scaling of topological defect creation in a second-order dynamical quantum phase transition, *New Journal of Physics* **12**, 095020 (2010).

[27] M. Uhlmann, R. Schützhold, and U. R. Fischer, $o(n)$ symmetry-breaking quantum quench: Topological defects versus quasiparticles, *Phys. Rev. D* **81**, 025017 (2010).

[28] A. Gambassi and P. Calabrese, Quantum quenches as classical critical films, *Europhysics Letters* **95**, 66007 (2011).

[29] J. Sak, Recursion relations and fixed points for ferromagnets with long-range interactions, *Phys. Rev. B* **8**, 281 (1973).

[30] M. C. Angelini, G. Parisi, and F. Ricci-Tersenghi, Relations between short-range and long-range ising models, *Phys. Rev. E* **89**, 062120 (2014).

[31] N. Defenu, A. Trombettoni, and A. Codello, Fixed-point structure and effective fractional dimensionality for $O(N)$ models with long-range interactions, *Phys. Rev. E* **92**, 052113 (2015).

[32] C. Behan, L. Rastelli, S. Rychkov, and B. Zan, A scaling theory for the long-range to short-range crossover and an infrared duality, *J. Phys. A* **50**, 354002 (2017).

[33] N. Defenu, A. Codello, S. Ruffo, and A. Trombettoni, *J. Phys. A Math. Gen.* **53**, 143001 (2020).

[34] P. W. Anderson and G. Yuval, Exact results in the kondo problem: Equivalence to a classical one-dimensional coulomb gas, *Phys. Rev. Lett.* **23**, 89 (1969).

[35] F. J. Dyson, Existence of a phase-transition in a one-dimensional ising ferromagnet, *Comm. Math. Phys.* **12**, 91 (1969).

[36] J. L. Cardy, One-dimensional models with $1/r^2$ interactions, *J. Phys. A* **14**, 1407 (1981).

[37] D. Benedetti, E. Lauria, D. Mazáč, and P. van Vliet, One-dimensional ising model with $1/r$ 1.99 interaction, *Physical Review Letters* **134**, 201602 (2025).

[38] V. Pagni, G. Giachetti, A. Trombettoni, and N. Defenu, One-dimensional long-range ising model: two (almost) equivalent approximations, *arXiv preprint arXiv:2510.02458* (2025).

[39] G. S. Joyce, Spherical model with long-range ferromagnetic interactions, *Phys. Rev.* **146**, 349 (1966).

[40] G. Giachetti, N. Defenu, S. Ruffo, and A. Trombettoni, Berezinskii–Kosterlitz–Thouless phase transitions with long-range couplings, *Phys. Rev. Lett.* **127**, 156801 (2021).

[41] S. Sachdev, *Quantum phase transitions*, Vol. 12 (IOP Publishing, 1999).

[42] N. Defenu, A. Trombettoni, and S. Ruffo, Anisotropic long-range spin systems, *Phys. Rev. B* **94**, 224411 (2016).

[43] A. Solfanelli and N. Defenu, Universality in long-range interacting systems: The effective dimension approach, *Physical Review E* **110**, 10.1103/physreve.110.044121 (2024).

[44] A. Campa, T. Dauxois, and S. Ruffo, Statistical mechanics and dynamics of solvable models with long-range interactions, *Phys. Rep.* **480**, 57 (2009).

[45] M. Kastner, Nonequivalence of ensembles for long-range quantum spin systems in optical lattices, *Phys. Rev. Lett.* **104**, 240403 (2010).

[46] N. Defenu, D. Mukamel, and S. Ruffo, Ensemble inequivalence in long-range quantum systems, *Phys. Rev. Lett.* **133**, 050403 (2024).

[47] M. Kastner, Nonequivalence of ensembles in the Curie–Weiss anisotropic quantum Heisenberg model, *JSTAT* **2010** (07), P07006.

[48] M. Moshe and J. Zinn-Justin, Quantum field theory in the large n limit: a review, *Physics Reports* **385**, 69–228 (2003).

[49] T. H. Berlin and M. Kac, The spherical model of a ferromagnet, *Physical Review* **86**, 821 (1952).

[50] M. Kac and C. J. Thompson, Spherical model and the infinite spin dimensionality limit, *Physica Norvegica* **5**, 163 (1971).

[51] B. Sciolla and G. Biroli, Quantum quenches, dynamical transitions, and off-equilibrium quantum criticality, *Phys. Rev. B* **88**, 201110 (2013).

[52] A. Chiocchetta, M. Tavora, A. Gambassi, and A. Mitra, Short-time universal scaling in an isolated quantum system after a quench, *Phys. Rev. B* **91**, 220302 (2015).

[53] A. Chiocchetta, M. Tavora, A. Gambassi, and A. Mitra, Short-time universal scaling and light-cone dynamics after a quench in an isolated quantum system in d spatial dimensions (2016).

[54] A. Maraga, A. Chiocchetta, A. Mitra, and A. Gambassi, Aging and coarsening in isolated quantum systems after a quench: Exact results for the quantum $O(n)$ model with $n \rightarrow \infty$, *Phys. Rev. E* **92**, 042151 (2015).

[55] G. Giachetti and N. Defenu, Entanglement propagation and dynamics in non-additive quantum systems, *Scientific Reports* **13**, 12388 (2023).

[56] H. J. Lipkin, N. Meshkov, and A. Glick, Validity of many-body approximation methods for a solvable model:(I). Exact solutions and perturbation theory, *Nuclear Physics* **62**, 188 (1965).

[57] A. Lerose, J. Marino, B. Žunkovič, A. Gambassi, and A. Silva, Chaotic dynamical ferromagnetic phase induced by nonequilibrium quantum fluctuations, *Phys. Rev. Lett.* **120**, 130603 (2018).

[58] A. Lerose, B. Žunkovič, J. Marino, A. Gambassi, and A. Silva, Impact of nonequilibrium fluctuations on prethermal dynamical phase transitions in long-range interacting spin chains, *Phys. Rev. B* **99**, 045128 (2019).

[59] G. Giachetti and N. Defenu, Conditions for quantum violent relaxation, *Physical Review B* **111**, 214301 (2025).

[60] S. Pappalardi, A. Russomanno, B. Žunkovič, F. Iemini, A. Silva, and R. Fazio, Scrambling and entanglement spreading in long-range spin chains, *Phys. Rev. B* **98**, 134303 (2018).

[61] S. Pappalardi, L. Foini, and J. Kurchan, Eigenstate thermalization hypothesis and free probability, *Phys. Rev. Lett.* **129**, 170603 (2022).

[62] G. Giachetti, A. Solfanelli, and N. Defenu, Universality and weak-ergodicity breaking in quantum quenches, *arXiv preprint arXiv:2511.08687* (2025).

[63] M. Kac, G. E. Uhlenbeck, and P. C. Hemmer, On the van der Waals Theory of the Vapor-Liquid Equilibrium. I. Discussion of a one-dimensional model, *JMP* **4**, 216 (1963).

[64] L. F. Cugliandolo, Out-of-equilibrium dynamics of classical and quantum complex systems, *Comptes Rendus Physique* **14**, 685 (2013), disordered systems / Systèmes désordonnés.

[65] A. Chandran, A. Nanduri, S. Gubser, and S. Sondhi, Equilibration and coarsening in the quantum $O(n)$ model at infinite n , *Phys. Rev. B* **88** (2013).

[66] C. Neumann, De problemate quodam mechanico, quod ad primam integralium ultraellipticorum classem revocatur, *Journal die reine und angewandte Mathematik (Crelle's Journal)* (1859).

[67] C. Neumann, *De problemate quodam mechanico, quod ad primam integralium ultraellipticorum classem revocatur: Dissertatio inauguralis* (Dalkowski, 1856).

[68] K. K. Uhlenbeck, Equivariant harmonic maps into spheres, in *Harmonic Maps: Proceedings of the NSF-CBMS Regional Conference, Held at Tulane University, New Orleans December 15–19, 1980* (Springer, 1982) pp. 146–158.

[69] D. Choodnovsky and G. Choodnovsky, Completely integrable class of mechanical systems connected with korteweg-de vries and multicomponent schrödinger equations-i, *Séminaire sur les équations non linéaires (Choodnovsky)*, 1 (1978).

[70] S. Wojciechowski, Integrability of one particle in a perturbed central quartic potential, *Physica Scripta* **31**, 433 (1985).

[71] L. F. Cugliandolo, G. S. Lozano, N. Nessi, M. Picco, and A. Tartaglia, Quenched dynamics of classical isolated systems: the spherical spin model with two-body random interactions or the neumann integrable model, *Journal of Statistical Mechanics: Theory and Experiment* **2018**, 063206 (2018).

[72] D. Barbier, L. F. Cugliandolo, G. S. Lozano, N. Nessi, M. Picco, and A. Tartaglia, Pre-asymptotic dynamics of the infinite size neumann ($p=2$ spherical) model, *Journal of Physics A: Mathematical and Theoretical* **52**, 454002 (2019).

[73] D. Barbier, L. F. Cugliandolo, G. S. Lozano, and N. Nessi, (non-equilibrium) thermodynamics of integrable models: The generalized gibbs ensemble description of the classical neumann model, *Europhysics Letters* **132**, 50002 (2020).

[74] D. Barbier, L. F. Cugliandolo, G. S. Lozano, and N. Nessi, Generalised Gibbs Ensemble for spherically constrained harmonic models, *SciPost Phys.* **13**, 048 (2022).

[75] A. Lerose and S. Pappalardi, Origin of the slow growth of entanglement entropy in long-range interacting spin systems, *Phys. Rev. Res.* **2**, 012041 (2020).

[76] C. G. J. Jacobi, *C. G. J. Jacobi's Vorlesungen über Dynamik: gehalten an der Universität zu Königsberg im Wintersemester 1842–1843 und nach einem von C. W. Borchardt ausgearbeiteten Hefte; herausgegeben von A. Clebsch*, 2nd ed. (G. Reimer, Berlin, 1884) edited by Alfred Clebsch; based on lecture notes by C. W. Borchardt.

[77] H. Casini and M. Huerta, Entanglement entropy in free quantum field theory, *J. Phys. A* **42**, 504007 (2009).

[78] P. Smacchia, M. Knap, E. Demler, and A. Silva, Exploring dynamical phase transitions and prethermalization with quantum noise of excitations, *Phys. Rev. B* **91**, 205136 (2015).